Finite-Element Analysis of Waveguide Modes: A Novel Approach That Eliminates Spurious Modes

TUPTIM ANGKAEW, MASANORI MATSUHARA, AND NOBUAKI KUMAGAI, FELLOW, IEEE

Abstract—**An efficient finite-element method for analyzing the propagation characteristics of a wide variety of waveguides is presented. A variational expression suited for the finite-element method is formulated in terms of the transverse electric and magnetic field components. In this approach, all guided-mode solutions are real, while the spurious-mode solutions are not real. Therefore, discrimination of the spurious-mode solutions can be achieved merely by imposing the simple condition that guided-mode solutions be real. Three numerical examples, two for the isotropic case and the other for the magnetic anisotropic case, are carried out.**

I. Introduction

RECENTLY, a method employing finite-element analysis to investigate the propagation characteristics of any arbitrarily shaped waveguide has attracted the attention of many researchers. The finite-element method is a powerful means which enables one to analyze a wide variety of waveguide problems. Several variational formulations for use with the finite-element method have been proposed [1]–[7]. Most of the variational expressions previously used are a functional of frequency and can be classified into the following three types [1]–[6]:

1) variational expressions which are formulated in terms of the longitudinal components of the electric field (e_z) and the magnetic field (h_z) and can be written as ω = functional (β, e_z, h_z) [1], [2];
2) variational expressions employing the longitudinal component (e_z) and the transverse component (e_t) of the electric field, which can be written as ω = functional (β, e_z, e_t) [3]; and
3) variational expressions employing all three components of the magnetic field, namely h_z and h_t, which can be written as ω = functional (β, h_z, h_t) [4]–[6].

Here, ω is the angular frequency and β is the propagation constant.

The most serious drawback associated with the finite-element method is the appearance of spurious-mode solutions. Up to this time, much effort has been devoted to finding a criterion to eliminate the spurious-mode solutions. A second drawback occurs in the application of variational expressions which are a functional of frequency. Let us consider, for example, the most common requirement in a waveguide problem, namely which mode can exist for a given value of frequency ω and what is the value for the propagation constant β? In order to fulfill this requirement, the calculation of the $\omega-\beta$ diagram must be performed. Further, if the permeability or permittivity of the medium is a function of frequency, the calculation becomes almost impossible.

The approaches proposed by Hano [3] and Koshiba *et al.* [6] are typical methods whereby the mixing of guided-mode solutions with the spurious-mode solutions is prevented. Hano has used a unique method that employs the variational expression of type 2, where the longitudinal and the transverse components of electric field are expressed as quadratic and linear functions of transverse coordinates, respectively. As a consequence of this approach, the values for ω of the spurious-mode solutions do not lie in the region of lower order guided modes. However, an overlap between the existence region of the values for ω^2 of the spurious-mode solutions and guided-mode solutions still occurs. Koshiba *et al.* have modified the variational expression of type 3 given in [4].[1] Besides the continuity condition for $i_z\cdot(n\times h_t)$ and $i_z\cdot h_z$ at the boundary between element and element, a supplementary boundary condition, which requires the continuity of $n\cdot h_t$, has been introduced. Consequently, the values for ω of the spurious-mode solutions do not lie in the existence region of slow guided modes. However, an overlap between the existence region of ω^2 of the spurious-mode solutions and guided-mode solutions cannot be avoided. The supplementary boundary condition also has a constraint which restricts the scope of applications to cases where the permeability of the medium is uniform.

In this paper, a finite-element formulation intended to overcome the two drawbacks previously mentioned is proposed. A novel variational expression is established in terms of the transverse electric and magnetic field components. In our finite-element program, we assign the parameters according to the necessary boundary conditions $i_z\cdot(n\times e_t)$ and $i_z\cdot(n\times h_t)$ required in the variational expres-

Manuscript received July 22, 1986; revised October 10, 1986.

The authors are with the Department of Electrical Communication Engineering, Osaka University, Yamada Oka, Suita, Osaka 565 Japan.

IEEE Log Number 8611939.

[1]Recently, Hayata *et al.* [7] have demonstrated a method more advanced than that outlined in [4].

0018-9480/87/0200-0117$01.00 ©1987 IEEE

sion. In our approach, the spurious-mode solutions are not real while the guided-mode solutions are real. Thus, the discrimination between spurious-mode solutions and guided-mode solutions can be achieved merely by imposing the simple condition that the latter be real. In addition to the advantage that the spurious-mode solutions can be eliminated, our method can also be applied to the case where the permeability or permittivity of the medium is a function of frequency. Therefore, our finite-element formulation is very useful for the analysis of arbitrarily shaped waveguides.

The application of our finite-element method to isotropic and anisotropic waveguides is discussed. In particular, the case where the permeability of the medium is a function of frequency is considered.

II. Variational Formulation in Terms of the Transverse Electromagnetic Field Components

Consider the anisotropic waveguide with an arbitrary cross section in the $x-y$ plane. The waveguide is assumed to be uniform along its longitudinal z-axis. Then the cross section of the waveguide is subdivided into a finite number of elements according to the finite-element method. The permittivity and permeability tensors of the anisotropic medium are assumed to be Hermite tensors and are defined in matrix form as

$$\epsilon = \begin{bmatrix} \epsilon_{tt} & \epsilon_{tz} \\ \epsilon_{zt} & \epsilon_{zz} \end{bmatrix} \quad \mu = \begin{bmatrix} \mu_{tt} & \mu_{tz} \\ \mu_{zt} & \mu_{zz} \end{bmatrix}$$

where the subscripts tt, tz, zt, and zz refer to 2×2, 2×1, 1×2, and 1×1 submatrices, respectively. From Maxwell's equations, the equations that govern the electromagnetic fields in each element are

$$\begin{aligned} &\omega\epsilon_{tt}\cdot\boldsymbol{e}_t + \omega\epsilon_{tz}\cdot\boldsymbol{e}_z + j\nabla\times\boldsymbol{h}_z + \beta\boldsymbol{i}_z\times\boldsymbol{h}_t = 0 \\ &\omega\mu_{tt}\cdot\boldsymbol{h}_t + \omega\mu_{tz}\cdot\boldsymbol{h}_z - j\nabla\times\boldsymbol{e}_z - \beta\boldsymbol{i}_z\times\boldsymbol{e}_t = 0 \end{aligned} \tag{1}$$

where $\boldsymbol{e}_t$ and $\boldsymbol{h}_t$ are the transverse components of the electric and magnetic fields, respectively. The longitudinal components, $\boldsymbol{e}_z$ and $\boldsymbol{h}_z$, can be expressed in terms of the transverse electromagnetic field components as

$$\begin{aligned} \boldsymbol{e}_z &= \frac{1}{j\omega\epsilon_{zz}}(\nabla\times\boldsymbol{h}_t - j\omega\epsilon_{zt}\cdot\boldsymbol{e}_t) \\ \boldsymbol{h}_z &= -\frac{1}{j\omega\mu_{zz}}(\nabla\times\boldsymbol{e}_t + j\omega\mu_{zt}\cdot\boldsymbol{h}_t). \end{aligned} \tag{2}$$

At the boundary of each element, the boundary conditions for the electromagnetic fields in (1) require the following.

For the boundary between element and element

$$\left.\begin{aligned} \boldsymbol{i}_z\cdot(\boldsymbol{n}\times\boldsymbol{e}_t) &= \text{continuous function} \\ \boldsymbol{i}_z\cdot\boldsymbol{e}_z &= \text{continuous function} \\ \boldsymbol{i}_z\cdot(\boldsymbol{n}\times\boldsymbol{h}_t) &= \text{continuous function} \\ \boldsymbol{i}_z\cdot\boldsymbol{h}_z &= \text{continuous function.} \end{aligned}\right\} \tag{3a}$$

For the boundary between element and electric wall

$$\boldsymbol{i}_z\cdot(\boldsymbol{n}\times\boldsymbol{e}_t) = 0, \quad \boldsymbol{i}_z\cdot\boldsymbol{e}_z = 0. \tag{3b}$$

For the boundary between element and magnetic wall

$$\boldsymbol{i}_z\cdot(\boldsymbol{n}\times\boldsymbol{h}_t) = 0, \quad \boldsymbol{i}_z\cdot\boldsymbol{h}_z = 0. \tag{3c}$$

Here, $\boldsymbol{n}$ is a normal unit vector to the boundary of each element.

Next, the guided-mode solutions that satisfy (1) and the boundary conditions in (3) make the following functional of propagation constant stationary. In other words, we can prove that this functional is a variational expression

$$\beta(\boldsymbol{e}_t, \boldsymbol{h}_t) = \sum A(\boldsymbol{e}_t, \boldsymbol{h}_t) \Big/ \sum B(\boldsymbol{e}_t, \boldsymbol{h}_t) \tag{4}$$

where

$$\begin{aligned} A(\boldsymbol{e}_t, \boldsymbol{h}_t) = \int \Bigg[& \boldsymbol{e}_t^*\cdot\omega\epsilon_{tt}\cdot\boldsymbol{e}_t + \boldsymbol{h}_t^*\cdot\omega\mu_{tt}\cdot\boldsymbol{h}_t \\ & - \frac{1}{\omega\mu_{zz}}(\nabla\times\boldsymbol{e}_t + j\omega\mu_{zt}\cdot\boldsymbol{h}_t)^* \\ & \cdot(\nabla\times\boldsymbol{e}_t + j\omega\mu_{zt}\cdot\boldsymbol{h}_t) \\ & - \frac{1}{\omega\epsilon_{zz}}(\nabla\times\boldsymbol{h}_t - j\omega\epsilon_{zt}\cdot\boldsymbol{e}_t)^* \\ & \cdot(\nabla\times\boldsymbol{h}_t - j\omega\epsilon_{zt}\cdot\boldsymbol{e}_t) \Bigg] ds \end{aligned}$$

$$B(\boldsymbol{e}_t, \boldsymbol{h}_t) = \int [\boldsymbol{i}_z\cdot(\boldsymbol{e}_t^*\times\boldsymbol{h}_t + \boldsymbol{e}_t\times\boldsymbol{h}_t^*)]\, ds.$$

Here, Σ denotes a summation taken over all elements and $\int ds$ denotes a surface integral taken in each element.

The trial functions of the transverse electric and magnetic field components used in (4) must necessarily satisfy the following boundary conditions at the boundary of each element.

For the boundary between element and element

$$\left.\begin{aligned} \boldsymbol{i}_z\cdot(\boldsymbol{n}\times\boldsymbol{e}_t) &= \text{continuous function} \\ \boldsymbol{i}_z\cdot(\boldsymbol{n}\times\boldsymbol{h}_t) &= \text{continuous function.} \end{aligned}\right\} \tag{5a}$$

For the boundary between element and electric wall

$$\boldsymbol{i}_z\cdot(\boldsymbol{n}\times\boldsymbol{e}_t) = 0. \tag{5b}$$

For the boundary between element and magnetic wall

$$\boldsymbol{i}_z\cdot(\boldsymbol{n}\times\boldsymbol{h}_t) = 0. \tag{5c}$$

In the following, we shall prove the validity of the variational expression in (4). First, we assume that the trial functions of the transverse electric and magnetic field components used in (4) differ from the true guided-mode solutions satisfying (1) and (3) by small admissible changes $\delta\boldsymbol{e}_t$ and $\delta\boldsymbol{h}_t$, respectively. Let $\delta\beta$ denote a variation of the propagation constant corresponding to $\delta\boldsymbol{e}_t$ and $\delta\boldsymbol{h}_t$. Under the condition that β and $\delta\beta$ be real, substituting the trial functions written in variation notations into (4) results in the following equations:

$$\delta\beta\sum B = \sum(A - \beta B) + \sum(\delta A - \beta\delta B) \tag{6}$$

where

$$A-\beta B=\int[\boldsymbol{e}_t^*\cdot(\omega\epsilon_{tt}\cdot\boldsymbol{e}_t+\omega\epsilon_{tz}\cdot\boldsymbol{e}_z+j\nabla\times\boldsymbol{h}_z+\beta\boldsymbol{i}_z\times\boldsymbol{h}_t)+\boldsymbol{h}_t^*\cdot(\omega\mu_{tt}\cdot\boldsymbol{h}_t+\omega\mu_{tz}\cdot\boldsymbol{h}_z-j\nabla\times\boldsymbol{e}_z-\beta\boldsymbol{i}_z\times\boldsymbol{e}_t)]\,ds+j\oint[\boldsymbol{h}_z\cdot(\boldsymbol{n}_0\times\boldsymbol{e}_t)^*-\boldsymbol{e}_z\cdot(\boldsymbol{n}_0\times\boldsymbol{h}_t)^*]\,dl \quad (7a)$$

and

$$\delta A-\beta\delta B=\int[\delta\boldsymbol{e}_t^*\cdot(\omega\epsilon_{tt}\cdot\boldsymbol{e}_t+\omega\epsilon_{tz}\cdot\boldsymbol{e}_z+j\nabla\times\boldsymbol{h}_z+\beta\boldsymbol{i}_z\times\boldsymbol{h}_t)+\delta\boldsymbol{h}_t^*\cdot(\omega\mu_{tt}\cdot\boldsymbol{h}_t+\omega\mu_{tz}\cdot\boldsymbol{h}_z-j\nabla\times\boldsymbol{e}_z-\beta\boldsymbol{i}_z\times\boldsymbol{e}_t)+\delta\boldsymbol{e}_t\cdot(\omega\epsilon_{tt}\cdot\boldsymbol{e}_t+\omega\epsilon_{tz}\cdot\boldsymbol{e}_z+j\nabla\times\boldsymbol{h}_z+\beta\boldsymbol{i}_z\times\boldsymbol{h}_t)^*+\delta\boldsymbol{h}_t\cdot(\omega\mu_{tt}\cdot\boldsymbol{h}_t+\omega\mu_{tz}\cdot\boldsymbol{h}_z-j\nabla\times\boldsymbol{e}_z-\beta\boldsymbol{i}_z\times\boldsymbol{e}_t)^*]\,ds+j\oint[\boldsymbol{h}_z\cdot(\boldsymbol{n}_0\times\delta\boldsymbol{e}_t)^*-\boldsymbol{e}_z\cdot(\boldsymbol{n}_0\times\delta\boldsymbol{h}_t)^*-\boldsymbol{h}_z^*\cdot(\boldsymbol{n}_0\times\delta\boldsymbol{e}_t)+\boldsymbol{e}_z^*\cdot(\boldsymbol{n}_0\times\delta\boldsymbol{h}_t)]\,dl. \quad (7b)$$

Here $\oint dl$ denotes a line integral taken along the entire boundary line in each element and $\boldsymbol{n}_0$ denotes an outward normal unit vector at the boundary of each element. The $\boldsymbol{e}_t$, $\boldsymbol{h}_t$, $\boldsymbol{e}_z$, $\boldsymbol{h}_z$, and β in (7) satisfy (1), (2), and (3). Thus, by substituting (1), (2), and (3) into (7) we get

$$\sum(A-\beta B)=0$$

$$\sum(\delta A-\beta\delta B)=\sum j\oint[\boldsymbol{h}_z\cdot(\boldsymbol{n}_0\times\delta\boldsymbol{e}_t)^*-\boldsymbol{e}_z\cdot(\boldsymbol{n}_0\times\delta\boldsymbol{h}_t)^*-\boldsymbol{h}_z^*\cdot(\boldsymbol{n}_0\times\delta\boldsymbol{e}_t)+\boldsymbol{e}_z^*\cdot(\boldsymbol{n}_0\times\delta\boldsymbol{h}_t)]\,dl. \quad (8)$$

Since $\delta\boldsymbol{e}_t$ and $\delta\boldsymbol{h}_t$ also satisfy the boundary conditions in (5) according to the trial functions $\boldsymbol{e}_t$ and $\boldsymbol{h}_t$, the term $\sum(\delta A-\beta\delta B)$ in the above equation becomes zero. Hence, (6) can be written as

$$\delta\beta=0. \quad (9)$$

From (9), we can prove that the functional in (4) is the variational expression accounting for (1) and (3). This variational expression has the advantage that for a given value of angular frequency, the values of the propagation constant can be obtained directly. The variational expression is also suited for a finite-element formulation in the sense that all guided-mode solutions are real while the spurious-mode solutions are not real. This is confirmed in the numerical examples described in Section IV.

III. Finite-Element Method

According to the standard finite-element method, the cross section of the waveguide is subdivided into a finite number of triangular elements. Fig. 1 shows an arbitrary triangular element. The node number and the corresponding node coordinate at each vertex are assigned as 1, (x_1, y_1), 2, (x_2, y_2), and 3, (x_3, y_3), respectively. The normal unit vector at each side is assigned as $\boldsymbol{n}_{12}$, $\boldsymbol{n}_{23}$, and $\boldsymbol{n}_{31}$ normal to, respectively, the sides (1–2), (2–3), and (3–1). The trial functions of the transverse electric and magnetic

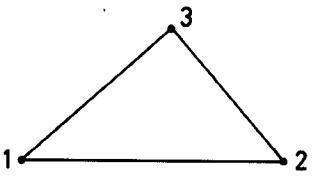

Fig. 1. An arbitrary triangular element.

field components in each element are expressed by using 12 unknown parameters as

$$\boldsymbol{e}_t=\sum_{m=1}^{6}\boldsymbol{N}_m(x,y)\phi_m$$

$$\boldsymbol{h}_t=\sum_{m=7}^{12}\boldsymbol{N}_{m-6}(x,y)\phi_m \quad (10)$$

where ϕ_m (for $m=1\sim12$) denotes unknown parameters and $\boldsymbol{N}_m(x, y)$ (for $m=1\sim6$) represents linear vector shape functions. The vector shape functions are determined by the scalar shape functions and the normal unit vectors in the element. These vector shape functions can be expressed as

$$\boldsymbol{N}_{2i-1}=\frac{\boldsymbol{n}_{ij}}{\boldsymbol{i}_z\cdot(\boldsymbol{n}_{ki}\times\boldsymbol{n}_{ij})}N_i$$

$$\boldsymbol{N}_{2i}=\frac{\boldsymbol{n}_{ki}}{\boldsymbol{i}_z\cdot(\boldsymbol{n}_{ij}\times\boldsymbol{n}_{ki})}N_i$$

$$N_i=\frac{(x_jy_k-x_ky_j)+(y_j-y_k)x+(x_k-x_j)y}{x_1y_2+x_2y_3+x_3y_1-x_2y_1-x_3y_2-x_1y_3} \quad (11)$$

where (i, j, k) permutes in a natural order. The equations for the unknown parameters ϕ_m (for $m=1\sim12$) can be recognized from (10) and (11) as follows

$$\phi_{2i-1}=\boldsymbol{i}_z\cdot(\boldsymbol{n}_{ki}\times\boldsymbol{e}_{ti})$$

$$\phi_{2i}=\boldsymbol{i}_z\cdot(\boldsymbol{n}_{ij}\times\boldsymbol{e}_{ti})$$

$$\phi_{2i+5}=\boldsymbol{i}_z\cdot(\boldsymbol{n}_{ki}\times\boldsymbol{h}_{ti})$$

$$\phi_{2i+6}=\boldsymbol{i}_z\cdot(\boldsymbol{n}_{ij}\times\boldsymbol{h}_{ti}) \quad (12)$$

where $\boldsymbol{e}_{ti}$ and $\boldsymbol{h}_{ti}$ (for $i=1\sim3$) denote the transverse electric and magnetic field components at node i. Equations (12) mean that the parameters ϕ_m (for $m=1\sim12$) are $\boldsymbol{i}_z\cdot(\boldsymbol{n}\times\boldsymbol{e}_t)$ and $\boldsymbol{i}_z\cdot(\boldsymbol{n}\times\boldsymbol{h}_t)$ taken at each side of the triangular element. By means of (12), the trial functions can be expressed in terms of parameters ϕ_m instead of explicitly using the transverse electric and magnetic field components. In this way, the trial functions can be forced to satisfy the necessary boundary conditions in (5) in a simple manner.

After substituting (10) into (4) and integrating, the following equations for A and B are obtained:

$$A=\phi^{*t}p\phi$$

$$B=\phi^{*t}q\phi. \quad (13)$$

Here, ϕ denotes a column vector composed of 12 unknown parameters used in the triangular element; p and q are

12×12 matrices composed of the values of permittivity, permeability, and vector shape functions in the element; and t denotes a transposed column vector.

Imposing the boundary conditions in (5) to (13) and summing over all elements, ΣA and ΣB are obtained. Then, substituting ΣA and ΣB into (4), the variational expression can be written as

$$\beta = \frac{\Phi^{*t} P \Phi}{\Phi^{*t} Q \Phi} \tag{14}$$

where Φ is a column vector composed of all unknown parameters used in the waveguide. P is a regular Hermitian matrix[2] and Q is a singular real symmetric matrix. The dimensions of P, Q, and Φ are exactly equal to six times the total number of elements in the case of linear shape functions.

The stationary condition of (4) requires the derivative of (14) with respect to Φ to be equal to zero. From this condition, we can obtain a generalized eigenvalue problem as

$$Q\Phi = \frac{1}{\beta} P\Phi \tag{15}$$

or, in detailed matrix form, as

$$\begin{bmatrix} 0 & Q_2 \\ Q_1 & 0 \end{bmatrix} \begin{bmatrix} \Phi_1 \\ \Phi_2 \end{bmatrix} = \frac{1}{\beta} \begin{bmatrix} P_1 & P_4 \\ P_3 & P_2 \end{bmatrix} \begin{bmatrix} \Phi_1 \\ \Phi_2 \end{bmatrix} \tag{16}$$

where Φ_1 and Φ_2 are subcolumn vectors of Φ composed of the unknown parameters used to express $\boldsymbol{e}_t$ and $\boldsymbol{h}_t$, respectively, in the waveguide. P_1, P_2, P_3, and P_4 are the submatrices of matrix P. Q_1 and Q_2 are the submatrices of matrix Q. For the common case where $\epsilon_{zt} = \mu_{zt} = 0$, the submatrices P_3 and P_4 become equal to zero and the following two equations can be obtained from (16):

$$Q_1\Phi_1 = \frac{1}{\beta} P_2\Phi_2 \tag{17}$$

$$Q_2\Phi_2 = \frac{1}{\beta} P_1\Phi_1. \tag{18}$$

From (17) and (18), we have

$$\left(P_1^{-1}Q_2P_2^{-1}Q_1\right)\Phi_1 = (1/\beta)^2\Phi_1 \tag{19}$$

$$\left(P_2^{-1}Q_1P_1^{-1}Q_2\right)\Phi_2 = (1/\beta)^2\Phi_2. \tag{20}$$

It is clear that one of the above two equations can be used to solve for β and that the dimension of both eigenvalue problems is approximately one half the dimension of (15). Thus, the eigenvalue problem obtained by using $\boldsymbol{e}_t$ and $\boldsymbol{h}_t$ can be reduced to an eigenvalue problem in which the unknown parameters are expressed only in terms of $\boldsymbol{e}_t$ or $\boldsymbol{h}_t$. It should also be mentioned that for the case where $\epsilon_{zt} \neq 0$ or $\mu_{zt} \neq 0$, (15) can be transformed into the standard eigenvalue problem: $P^{-1}Q\Phi = 1/\beta\Phi$.

By solving the eigenvalue problem, the eigenvectors Φ and the eigenvalues β are obtained. Substituting the eigenvectors into (10), we obtain the eigenfunctions of the transverse electric and magnetic field components. Thus, by following this method, we can calculate the electromagnetic field distribution in the waveguide.

IV. Numerical Examples and Considerations

A. Dielectric-Loaded Waveguide

As a first numerical example of the method described in Sections II and III, we investigate a dielectric-loaded waveguide. Fig. 2 shows the cross section of the dielectric-loaded waveguide of size $a\times2a$ bounded by a perfect conductor. Half of the waveguide is filled with dielectric material whose relative permittivity and permeability are equal to 2.25 and 1, respectively. The other half of the waveguide is assumed to be vacuum. The dielectric-loaded waveguide is a test case for the finite-element method, which is widely used in many papers, such as [3] and [6].

Now let us consider our result at, for example, $k_0a = \omega\sqrt{\epsilon_0\mu_0}\,a = 3$, where the cross section of the dielectric-loaded waveguide is subdivided into 64 triangular elements, as shown in Fig. 3. Here, k_0, ϵ_0, and μ_0 are the wavenumber, permittivity, and permeability in free space, respectively.

The total number of eigenvalues obtained with our method is equal to six times the total number of elements used in the finite-element mesh. Thus, for the present case, the total number of eigenvalues is equal to $64\times6 = 384$. These eigenvalues can be expressed in the form

$$k_0/\beta = u + jv \qquad (u, v \text{ real}).$$

All 384 eigenvalues can be classified into four types, as shown in Table I. From the eigenvalues in Table I, we may conclude that the eigenvalues of types 1, 2, and 3 are definitely nonphysical spurious-mode solutions, because these eigenvalues are not bounded real numbers. All eigenvalues of type 4 are real, as shown in the following:

$$\frac{\beta}{k_0} = \begin{cases} \pm1.27102 \text{ (the corresponding exact solution is } \pm1.27576) \\ \pm0.94546 \text{ (the corresponding exact solution is } \pm0.97154) \\ \pm0.67683 \text{ (the corresponding exact solution is } \pm0.72865) \\ \pm0.55718 \text{ (the corresponding exact solution is } \pm0.59390). \end{cases}$$

The eigenvalues of type 4 clearly represent the approximate values of the exact guided-mode solutions, and we also observe the one-to-one correspondence between the values of type 4 and the exact solutions. The positive and negative values of β in type 4 can be regarded as the

[2] In the case of isotropic and some anisotropic waveguides, P can be reduced to a real symmetric matrix.

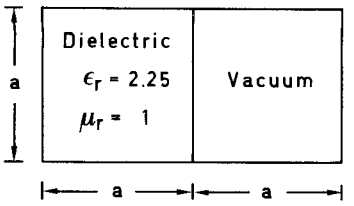

Fig. 2. The cross section of a dielectric-loaded waveguide.

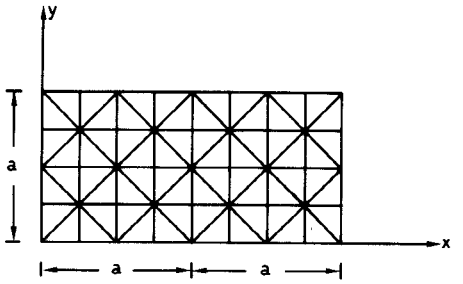

Fig. 3. Illustration of the finite-element division of a dielectric-loaded waveguide.

TABLE I
CLASSIFICATION OF 384 EIGENVALUES IN THE FINITE-ELEMENT ANALYSIS OF THE DIELECTRIC-LOADED WAVEGUIDE IN FIG. 3

Type 1	u = 0	v = 0	132 values
Type 2	u ≈ 0	v ≠ 0	240 values
Type 3	u ≃ 0	v ≠ 0	4 values
Type 4	u ≠ 0	v = 0	8 values

values corresponding to the waves propagating in $+z$ and $-z$ directions, respectively. Thus, if the condition that guided-mode solutions be real is imposed, all the spurious-mode solutions can be completely discriminated.

The finite-element analysis for the dielectric-loaded waveguide in Fig. 3 has been carried out by using a mesh with 64 triangular elements. In Fig. 4, the solid lines represent the finite-element analysis, while dots show the exact solutions. In case of the fundamental mode, our finite-element analysis agrees almost exactly with the exact solutions. The higher order modes, obviously, cannot be reproduced so well because of an insufficient number of elements in the finite-element mesh. However the accuracy in the higher order modes can be improved by increasing the number of elements or using quadratic shape functions instead of linear shape functions. Note that the cutoff frequency of each mode in Fig. 4 is the extrapolated value from the values near the cutoff frequency.

B. Ferrite-Loaded Waveguide

As a numerical example for the magnetic anisotropic case, we investigate a ferrite-loaded waveguide, shown in Fig. 5. The ferrite-loaded waveguide is a version of a nonreciprocal microwave components in which a ferrite

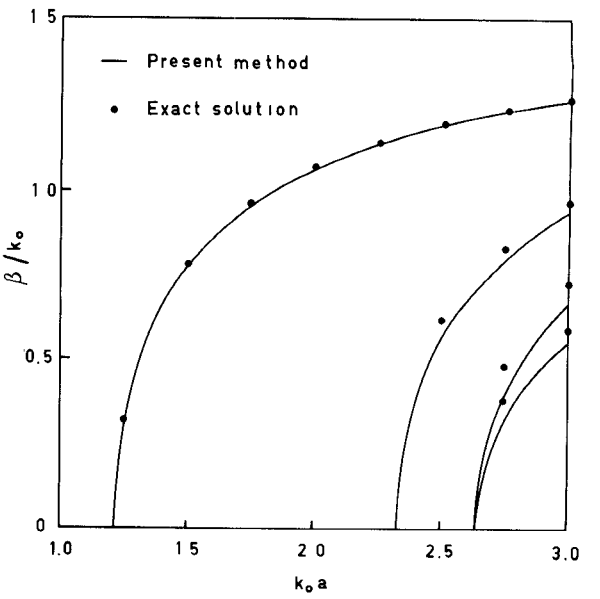

Fig. 4. Dispersion characteristics for a dielectric-loaded waveguide.

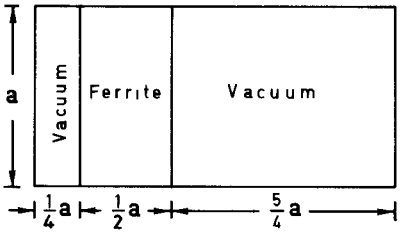

Fig. 5. The cross section of a ferrite-loaded waveguide.

slab is placed asymmetrically into the waveguide, and the static magnetic field is imposed transverse to the direction of propagation. The ferrite slab in the waveguide can be characterized by the tensor permeability $\bar{\mu}$ and the scalar permittivity ϵ as

$$\bar{\mu} = \begin{bmatrix} \mu & 0 & j\kappa \\ 0 & \mu_0 & 0 \\ -j\kappa & 0 & \mu \end{bmatrix}$$

$$\mu = \mu_0\left(1 + \frac{\omega_m\omega_0}{\omega_0^2 - \omega^2}\right)$$

$$\kappa = \mu_0\frac{\omega_m\omega}{\omega_0^2 - \omega^2}$$

$$\omega_0\sqrt{\epsilon_0\mu_0}\,a = \omega_m\sqrt{\epsilon_0\mu_0}\,a = 0.5$$

$$\epsilon = 10\epsilon_0.$$

Here, μ_0 and ϵ_0 are the permeability and permittivity in free space, respectively. The tensor permeability of the ferrite is frequency-dependent. Thus, the ferrite-loaded waveguide can be regarded as a proof for the validity of the finite-element method for the general case where the permeability of the medium is a function of frequency. For the case of the variational expression in (4), the finite-element analysis of the ferrite-loaded waveguide can be

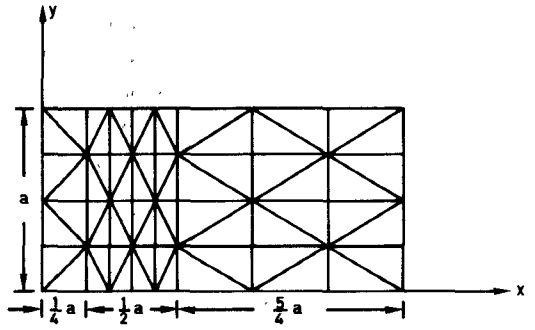

Fig. 6. Illustration of the finite-element division of a ferrite-loaded waveguide.

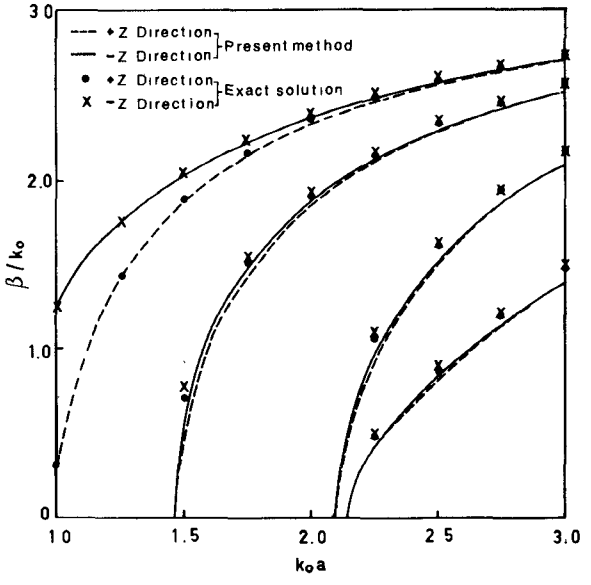

Fig. 7. Dispersion characteristics for a ferrite-loaded waveguide.

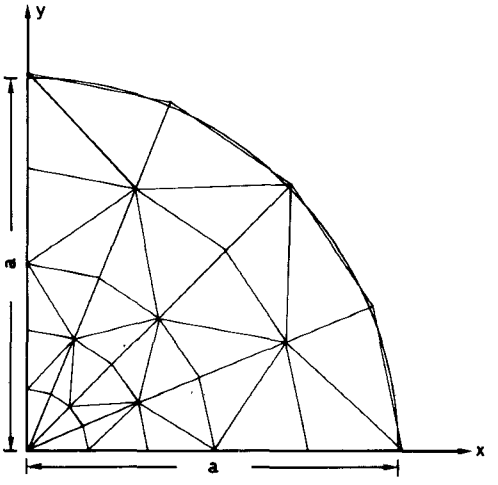

Fig. 8. Illustration of the finite-element division of one quarter of a hollow circular waveguide.

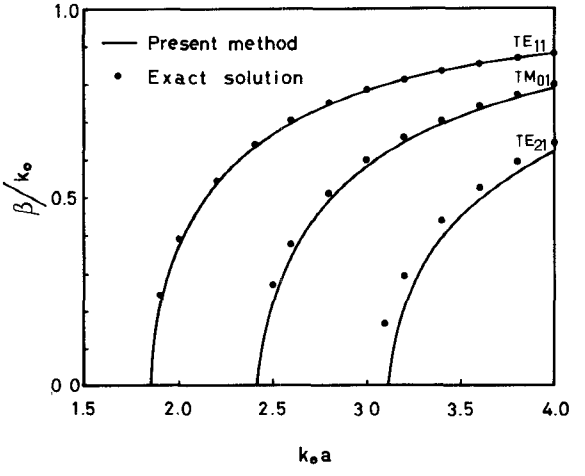

Fig. 9. Dispersion characteristics for a hollow circular waveguide.

accomplished because this variational expression is not a functional of frequency.

In Fig. 6, the cross section of the ferrite-loaded waveguide is subdivided into 64 triangular elements. The calculations are carried out by employing the finite-element mesh shown in Fig. 6. In Fig. 7, the dashed lines and solid lines represent the finite-element analysis corresponding to the waves propagating in the $+z$ and $-z$ directions, respectively, while the exact solutions are represented by dots and crosses. Again, our finite-element analysis is in good agreement with the exact solutions for the fundamental mode, but as in the numerical example of a dielectric-loaded waveguide previously discussed, deviations in the higher order modes still occur. The cause of the deviations in the higher order modes lies in the insufficient number of elements and in the circumstance that the shape functions being used do not yield the correct approximate functions fitted to the electromagnetic field distribution.

Note also that for the case of a ferrite-loaded waveguide, all spurious-mode solutions are not real while all guided-mode solutions are real. Thus, again, all spurious-mode solutions can be discriminated by imposing the condition that the guided-mode solutions be real.

C. Hollow Circular Waveguide

An additional numerical example has been carried out with a hollow circular waveguide. This example can be regarded as a test case with curved boundary. The computation is carried out with the mesh in Fig. 8, where a quarter of the waveguide is considered. A one-to-one correspondence between the real eigenvalues in our method and exact solutions has been observed, and no spurious-mode solutions appear to be real numbers. Fig. 9 shows the dispersion characteristics for the hollow circular waveguide. The solid lines and dots show the finite-element solutions and the exact solutions, respectively. Thus, the validity of the present method is also confirmed by this example.

V. Conclusions

A variational expression of the propagation constant, employing transverse electric and magnetic field components has been formulated and used in a finite-element method in order to investigate the propagation characteristics of waveguides. The trial functions of the transverse

electric and magnetic field components, which are expressed in terms of the unknown parameters according to the vector products. $\boldsymbol{i}_z \cdot (\boldsymbol{n} \times \boldsymbol{e}_t)$ and $\boldsymbol{i}_z \cdot (\boldsymbol{n} \times \boldsymbol{h}_t)$, were used in this finite-element method. A complete discrimination of the spurious-mode solutions from guided-mode solutions was confirmed by imposing the simple condition that the guided-mode solutions be real. This simple condition does not appear to be available in any of the variational expressions previously proposed. Numerical examples are given for a dielectric-loaded waveguide, ferrite-loaded waveguide, and hollow circular waveguide.

REFERENCES

[1] C. Yeh, K. Ha, S. B. Dong, and W. P. Brown, "Single-mode optical waveguides," *Appl. Opt.*, vol. 18, pp. 1490–1504, May 1979.

[2] K. Oyamada and T. Okoshi, "Two-dimensional finite-element method calculation of propagation characteristics of axially nonsymmetrical optical fibers," *Radio Sci.*, vol. 17, pp. 109–116, Jan.–Feb. 1982.

[3] M. Hano, "Finite-element analysis of dielectric-loaded waveguides," *IEEE Trans. Microwave Theory Tech.*, vol. MTT-32, pp. 1275–1279, Oct. 1984.

[4] A. Konrad, "High-order triangular finite elements for electromagnetic waves in anisotropic media," *IEEE Trans. Microwave Theory Tech.*, vol. MTT-25, pp. 353–360, May 1977.

[5] B. M. A. Rahman and J. B. Davies, "Penalty function improvement of waveguide solution by finite elements," *IEEE Trans. Microwave Theory Tech.*, vol. MTT-32, pp. 922–928, Aug. 1984.

[6] M. Koshiba, K. Hayata, and M. Suzuki, "Improved finite-element formulation in terms of the magnetic field vector for dielectric waveguides," *IEEE Trans. Microwave Theory Tech.*, vol. MTT-33, pp. 227–233, Mar. 1985.

[7] K. Hayata, M. Koshiba, M. Eguchi, and M. Suzuki, "Novel finite-element formulation without any spurious solutions for dielectric waveguides," *Electron. Lett.*, vol. 22, pp. 295–296, Mar. 1986.

Tuptim Angkaew was born in Bangkok, Thailand, on November 9, 1961. She received the B.Eng. in electrical engineering from King Mongkut's Institute of Technology, Ladkrabang Campus, Bangkok, in 1984. Since 1985, she has been working toward the M.S. degree at the Department of Communication Engineering, Faculty of Engineering, Osaka University, Japan.

Masanori Matsuhara graduated from Fukui University, Department of Electrical Engineering, in 1963, and in 1968 he completed the doctoral course in communication engineering at Osaka University.

In 1968, he joined the Faculty of Engineering at Osaka University as an Assistant Professor. In 1972, he was promoted to Associate Professor. Dr. Matsuhara's research interests center on optical waveguides and optical integrated circuits. His publications include the book *Modern Electromagnetic Theory*.

Nobuaki Kumagai (M'59–SM'71–F'81) was born in Japan on May 19, 1929. He received the B. Eng. and D. Eng. degrees from Osaka University, Osaka, Japan, in 1953 and 1959, respectively.

From 1956 to 1960, he was a Research Associate in the Department of Communication Engineering at Osaka University. From 1958 through 1960, he was a Visiting Senior Research Fellow at the Electronics Research Laboratory of the University of California, Berkeley, while on leave of absence from Osaka University. From 1960 to 1970, he was an Associate Professor of Communication Engineering at Osaka University, and in 1971 he became a Professor. From 1980 to 1982, he served as Dean of Students at Osaka University. In April 1985, he was named Dean of Engineering of Osaka University, and he has been President of the university since August 1985. His fields of interest are electromagnetic theory and its applications to microwave, millimeter-wave, and acoustic-wave engineering, optical fibers and related techniques, and lasers and their applications. He has published more than 100 technical papers on these topics in various journals.

Dr. Kumagai is the author or coauthor of several books, including *Microwave Circuits* and *Introduction to Relativistic Electromagnetic Field Theory*. From 1979 to 1981, he was Chairman of the technical group on Microwave Theory and Techniques of the Institute of Electronics and Communication Engineers of Japan. He is a member of the Telecommunications Technology Council of the Ministry of Post and Telecommunications and is a consultant for the Nippon Telegraph and Telephone Corporation (NTT). Dr. Kumagai is Vice President of the Institute of Electronics and Communication Engineers of Japan and is a member of the Institute of Electrical Engineers of Japan and of the Laser Society of Japan. He has received the Achievement Award from the Institute of Electronics and Communication Engineers of Japan and the Special Award from the Laser Society of Japan. He was also awarded an IEEE Fellowship for contributions to the study of wave propagation in electromagnetics, optics, and acoustics.